EIGENSTATE THERMALIZATION HYPOTHESIS IN THE DICKE MODEL

6th Annual Meeting:

Chaos and Thermalization in Quantum Many-Body Systems

David Villaseñor

IIMAS-UNAM

January 19-22, 2023

Collaborators

- Jorge G. Hirsch, ICN-UNAM, CDMX.
- Lea F. Santos, University of Connecticut, Storrs, USA.
- Sergio Lerma-Hernández, UV, Xalapa, Veracruz.
- Miguel A. Bastarrachea-Magnani, UAM-Iztapalapa, CDMX.
- Saúl Pilatowsky-Cameo, MIT, Cambridge, USA.




Outline

Introduction

Evolution of a pure state $|\Psi(0)\rangle = \sum_k c_k |E_k\rangle$ under a Hamiltonian $\hat{H}$:

$$|\Psi(t)\rangle = e^{-i\hat{H}t}|\Psi(0)\rangle = \sum_k c_k e^{-iE_k t}|E_k\rangle \tag{1}$$

- Eigenvalue equation: $\hat{H}|E_k\rangle = E_k|E_k\rangle$
- Coefficients: $c_k = \langle E_k|\Psi(0)\rangle$

Evolution of a given operator $\hat{O}$:

$$O(t) = \langle\Psi(t)|\hat{O}|\Psi(t)\rangle = \sum_{k\neq k'} c_k^* c_{k'} e^{i(E_k - E_{k'})t} O_{k,k'} + \sum_k |c_k|^2 O_{k,k} \tag{2}$$

- Matrix elements: $O_{k,k'} = \langle E_k|\hat{O}|E_{k'}\rangle$

Infinite-time average of a given operator $\hat{O}$:

$$\bar{O} = \lim_{t \to +\infty} \frac{1}{t} \int_0^t dt' O(t') = \sum_k |c_k|^2 O_{k,k} \tag{3}$$

- Diagonal matrix elements: $O_{k,k} = \langle E_k | \hat{O} | E_k \rangle$

Microcanonical average of a given operator $\hat{O}$:

$$O_{\text{mic}} = \frac{1}{W_{E,\Delta E}} \sum_k O_{k,k} \tag{4}$$

- Energy window: $E_k \in (E - \Delta E, E + \Delta E)$

Eigenstate thermalization hypothesis (ETH):

- Diagonal ETH: $\bar{O} \approx O_{\text{mic}}$ when system size increases.
- Off-diagonal ETH: Fluctuations around $\bar{O}$ decrease and cancel out on average when system size increases.

Deviations from microcanonical average (diagonal ETH):

$$\Delta^{\text{mic}}[O] = \frac{\sum_k |O_{k,k} - O_{\text{mic}}|}{\sum_k O_{k,k}} \tag{5}$$

$$\Delta_{\text{e}}^{\text{mic}}[O] = \left| \frac{\max(O) - \min(O)}{O_{\text{mic}}} \right| \tag{6}$$

Observable with N non-zero eigenvalues (diagonal and off-diagonal ETH):

$$O_{k,k} = \langle E_k|\hat{O}|E_k\rangle = \sum_{n=1}^{N} |C_{O_n}^k|^2 \langle O_n|\hat{O}|O_n\rangle \tag{7}$$

$$O_{k,k'} = \langle E_k|\hat{O}|E_{k'}\rangle = \sum_{n=1}^{N} (C_{O_n}^k)^* C_{O_n}^{k'} \langle O_n|\hat{O}|O_n\rangle \tag{8}$$

- Eigenvalue equation: $\hat{O}|O_n\rangle = O_n|O_n\rangle$
- Eigenstates: $|E_k\rangle = \sum_n C_{O_n}^k |O_n\rangle$
- Central limit theorem: A large sum of independent random numbers follows a Gaussian distribution.

Spin-Boson Dicke Model

Hamiltonian of the Dicke model:

$$\hat{H}_{\mathrm{D}} = \omega \hat{a}^{\dagger}\hat{a} + \omega_0 \hat{J}_z + \frac{2\gamma}{\sqrt{\mathcal{N}}}\hat{J}_x(\hat{a}^{\dagger} + \hat{a}) \tag{9}$$

- Field operators: $\hat{a}$ ($\hat{a}^{\dagger}$)
- Atomic operators: $\hat{J}_{x,y,z} = \sum_{n=1}^{\mathcal{N}} \hat{\sigma}^{n}_{x,y,z}/2$
- Parameters: $\mathcal{N} = 2j$, ω, ω_0, γ
- QPT at $\gamma_{\mathrm{c}} = \sqrt{\omega\omega_0}/2$: normal ($\gamma < \gamma_{\mathrm{c}}$) and super-radiant ($\gamma > \gamma_{\mathrm{c}}$) phase

Classical limit of the Dicke model:

$$h_{\mathrm{D}}(\mathbf{x}) = \frac{\langle \mathbf{x}|\hat{H}_{\mathrm{D}}|\mathbf{x}\rangle}{j} = \frac{\omega}{2}\left(q^2+p^2\right) + \frac{\omega_0}{2}\left(Q^2+P^2\right) - \omega_0 + 2\gamma q Q\sqrt{1-\frac{Q^2+P^2}{4}} \tag{10}$$

- Glauber-Bloch coherent states: $|\mathbf{x}\rangle = |q,p\rangle \otimes |Q,P\rangle$, $|q,p\rangle = \hat{D}(q,p)|0\rangle$, $|Q,P\rangle = \hat{R}(Q,P)|j,-j\rangle$
- Canonical variables: $\mathbf{x} = (q,p;Q,P)$
- Scaled energy shells: $\epsilon = E/j$

Chaos in the Spin-Boson Dicke Model

Indicators of chaos:

- Classical chaos: Poincaré section, Lyapunov exponent, map of percentage of chaos
- Quantum chaos: Energy level statistics, ratio of consecutive energy levels $\langle \widetilde{r} \rangle$, Peres lattice, correlation hole, OTOC

Ratio of consecutive energy levels:

$$\widetilde{r}_k = \min\left(r_k, \frac{1}{r_k}\right) = \frac{\min(s_k, s_{k-1})}{\max(s_k, s_{k-1})} \tag{11}$$

- Nearest-neighbor spacing: $s_k = E_{k+1} - E_k$
- $r_k = s_k / s_{k-1}$

- D. Villaseñor, S. Pilatowsky-Cameo, M. A. Bastarrachea-Magnani, S. Lerma-Hernández, L. F. Santos, and J. G. Hirsch, Entropy **25**, 8 (2023).

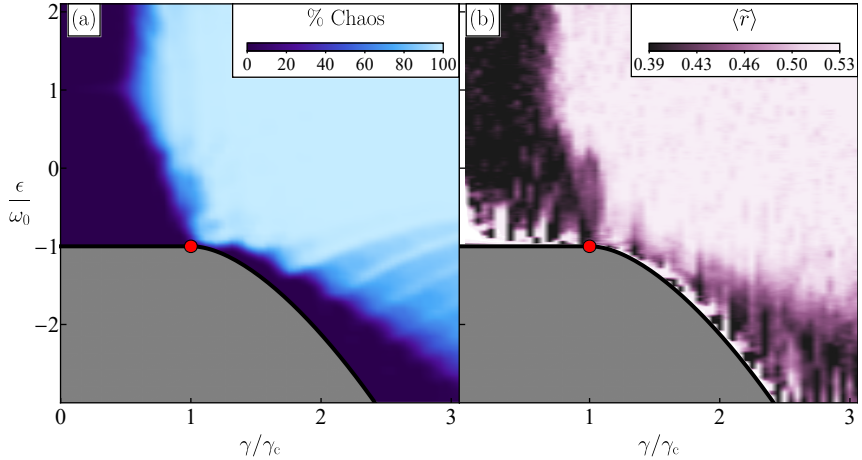

Figure: Map of percentage of chaos (a) and map of average values of ratio $\langle \tilde{r} \rangle$ (b). System size in panel (b): $j = 100$.

Thermalization in the Spin-Boson Dicke Model

Expectation values of number of photons and exited atoms:

$$n_{k,k} = \langle E_k|\hat{n}|E_k\rangle = \langle E_k|\hat{a}^\dagger\hat{a}|E_k\rangle \tag{12}$$

$$(n_{\text{ex}})_{k,k} = \langle E_k|\hat{n}_{\text{ex}}|E_k\rangle = \langle E_k|(\hat{J}_z + j\hat{1})|E_k\rangle \tag{13}$$

- D. Villaseñor, S. Pilatowsky-Cameo, M. A. Bastarrachea-Magnani, S. Lerma-Hernández, L. F. Santos, and J. G. Hirsch, Entropy **25**, 8 (2023).

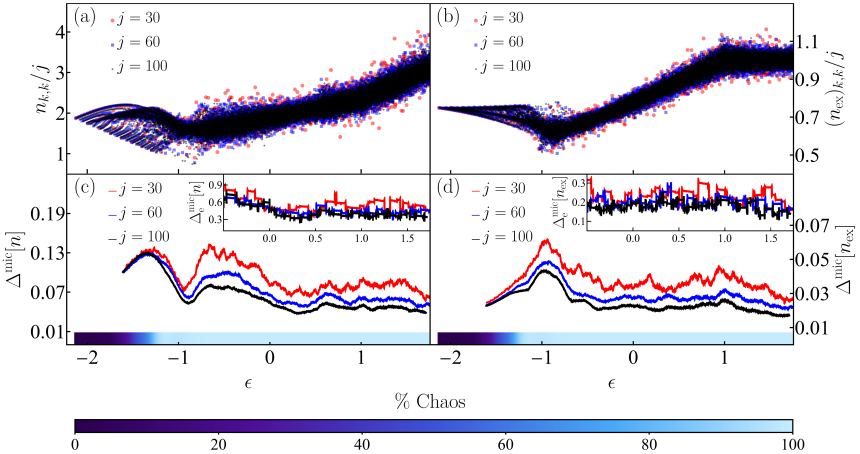

Figure: Peres lattice of expectation values for number of photons (a) and excited atoms (b). Deviations from microcanonical average for number of photons (c) and excited atoms (d). System size: $j = 30, 60, 100$.

- D. Villaseñor, S. Pilatowsky-Cameo, M. A. Bastarrachea-Magnani, S. Lerma-Hernández, L. F. Santos, and J. G. Hirsch, Entropy **25**, 8 (2023).

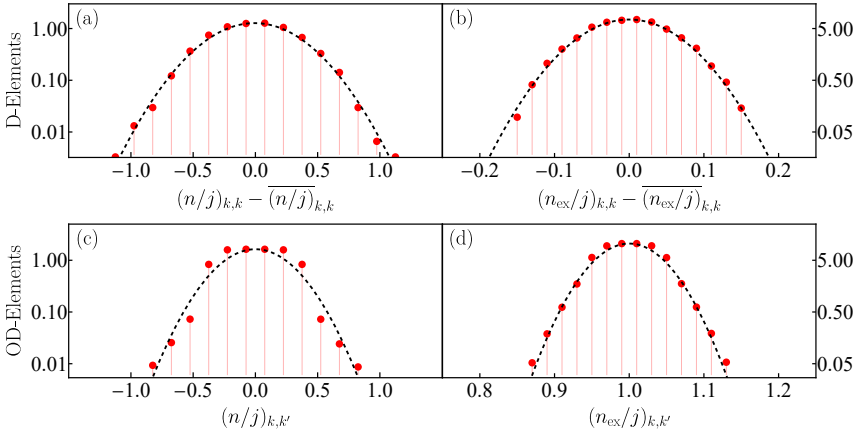

Figure: Statistical distribution of matrix elements for number of photons [diagonal (a), off-diagonal (c)] and excited atoms [diagonal (b), off-diagonal (d)]. System size: $j = 30$.

Von Neumann entanglement entropy:

$$S_{\mathrm{En}} = -\mathrm{Tr}[\hat{\rho}_{\mathrm{A}} \ln(\hat{\rho}_{\mathrm{A}})] \tag{14}$$

- Bipartite Hilbert space: $\mathcal{H}_{\mathrm{D}} = \mathcal{H}_{\mathrm{A}} \otimes \mathcal{H}_{\mathrm{B}}$
- Atomic reduced density matrix: $\hat{\rho}_{\mathrm{A}} = \mathrm{Tr}_{\mathrm{B}}[\hat{\rho}]$
- Density matrix (pure state): $\hat{\rho} = |\Psi\rangle\langle\Psi|$
- State expanded in Fock basis: $|\Psi\rangle = \sum_{n=0}^{\infty} \sum_{m_z=-j}^{j} c_{n,m_z} |n; j, m_z\rangle$

- D. Villaseñor, S. Pilatowsky-Cameo, M. A. Bastarrachea-Magnani, S. Lerma-Hernández, L. F. Santos, and J. G. Hirsch, Entropy **25**, 8 (2023).

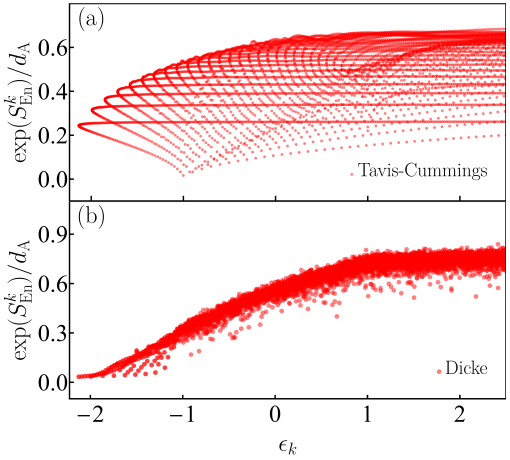

Figure: Peres lattice of exponential of von Neumann entanglement entropy for eigenstates of an integrable (a) and non-integrable (b) model. System size: $j = 30$.

- D. Villaseñor, S. Pilatowsky-Cameo, M. A. Bastarrachea-Magnani, S. Lerma-Hernández, L. F. Santos, and J. G. Hirsch, Entropy **25**, 8 (2023).

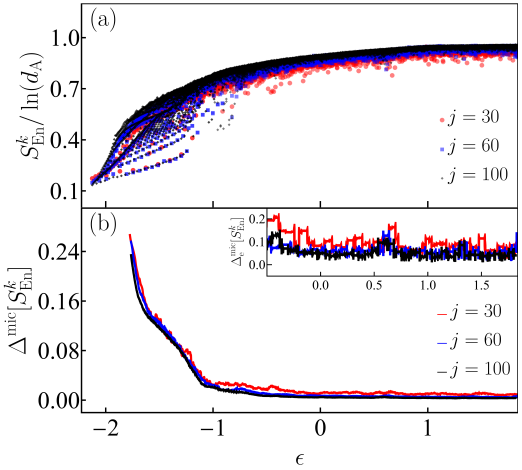

Figure: Peres lattice of von Neumann entanglement entropy for eigenstates (a) and deviations from microcanonical average (b). System size: $j = 30, 60, 100$.

Shannon entropy:

$$S_{\mathrm{Sh}} = -\sum_{x=0}^{\infty} \sum_{y=-j}^{j} |c_{x,y}|^2 \ln(|c_{x,y}|^2) \tag{15}$$

- State expanded in arbitrary basis: $|\Psi\rangle = \sum_{x=0}^{\infty} \sum_{y=-j}^{j} c_{x,y} |x; j, y\rangle$
- Fock basis: $(x, y) = (n, m_z)$
- Efficient basis: $(x, y) = (N, m_x)$

- D. Villaseñor, S. Pilatowsky-Cameo, M. A. Bastarrachea-Magnani, S. Lerma-Hernández, L. F. Santos, and J. G. Hirsch, Entropy **25**, 8 (2023).

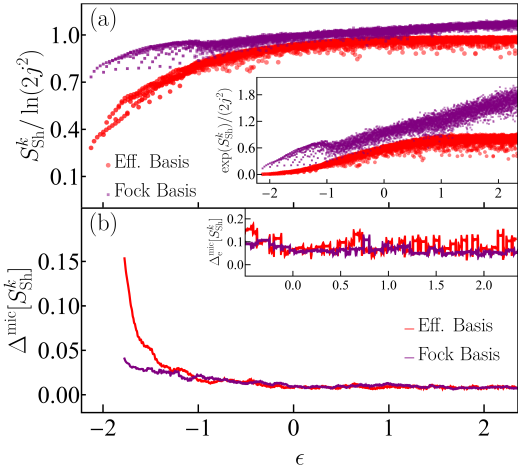

Figure: Peres lattice of Shannon entropy for eigenstates (a) and deviations from microcanonical average (b) in two diagonalization bases. System size: $j = 30$.

- D. Villaseñor, S. Pilatowsky-Cameo, M. A. Bastarrachea-Magnani, S. Lerma-Hernández, L. F. Santos, and J. G. Hirsch, Entropy **25**, 8 (2023).

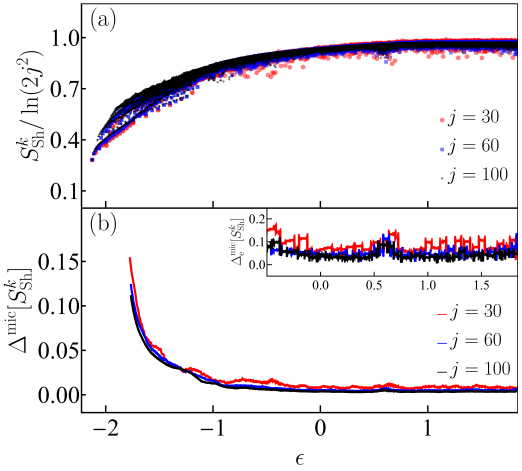

Figure: Peres lattice of Shannon entropy for eigenstates (a) and deviations from microcanonical average (b). System size: $j = 30, 60, 100$.

Conclusions

- The ETH was confirmed in the chaotic region of the Dicke model using expectation values of number of photons and excited atoms for different system sizes.
- The study of diagonal and off-diagonal matrix elements of these expectation values showed Gaussian distributions, which indicates that the eigenstates behave as random vectors and are chaotic.
- The use of entropies to validate the ETH showed a better reduction of the deviations from the microcanonical average.
- The Shannon entropy made evident the advantage of using the so-called efficient basis over the Fock basis reaching more converged states for larger systems sizes, since the former tends to saturate, while the latter tends to grow up indefinitely.